ChemComm

Accepted Manuscript

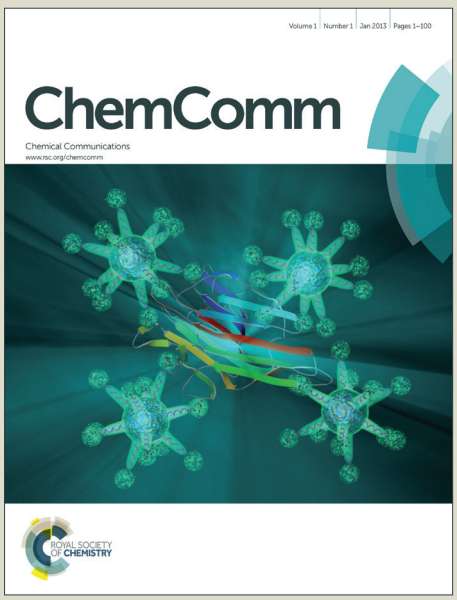

ROYAL SOCIETY OF CHEMISTRY

www.rsc.org/chemcomm

Journal Name

COMMUNICATION

A High Stiffness Bio-inspired Hydrogel from the Combination of Poly (amido amine) Dendrimer with DOPA

Received 00th January 20xx,

Yao Wang,[ab] Qiang Zhao,[ac] Yiyang Luo,[ab] Zejun Xu,[ab] He Zhang,[d] Sheng Yang,*[d] Yen Wei,[e] and Xinru Jia*[ab]

Accepted 00th January 20xx

DOI: 10.1039/x0xx00000x

www.rsc.org/

A robust biodegradable hydrogel is constructed from the two components containing G4.0 PAMAM and DOPA, which displays excellent interconnected porous 3D networks, higher mechanical strength, low and stable swelling and well biocompatibility. Mouse CSD model in vivo evidences that moderate bone-like tissue and extensive bony tissue are observed when the hydrogel implanted.

Hydrogels either from naturally derived polymers[1] or synthetic polymers[2] are the certain promising materials in a diverse range of applications including tissue repair,[3] drug delivery[4] and regenerative medicine.[5] The superiorities of hydrogels from natural polymers are their high biocompatibility and the structural resemblance to other macromolecules found in the body, which enable them to simulate native tissue microenvironments.[6] In comparison, the hydrogels from synthetic polymers are known with the advantages of modifiable chemical structures and tunable properties. However, the inherent weak mechanical strength, poor deformability, unstable swelling feature and lack of bioactivity are the crucial defects, thus leading to severe restriction of their biomedical applications.[7] To improve the situation, a variety of hydrogel systems have been developed in recent years, such as topological (TP) gels,[8] nanocomposite gels,[9] double-network (DN) gels,[10] polymer-peptide gels,[11] macromolecular microsphere composite (MMC) hydrogels,[12] etc.

Recent studies revealed that a bio-inspired ingredient from mussel, 3, 4-dihydroxy-L-phenylalanine (DOPA),[13] displayed a remarkable effect on reinforcing hydrogel's strength and performed chemical multifunctionality to adhere on varied substrates from organic to metallic. This gives a new picture of constructing biocompatible hydrogels with desirable physical properties. A series of reports have been presented by P. B. Messersmith et al., who demonstrated that the incorporation of DOPA allowed constructing adhesive hydrogels with high toughness.[14]

Poly (amido amine) (PAMAM) dendrimers are considered as one of the most promising polymer architectures in biomedical

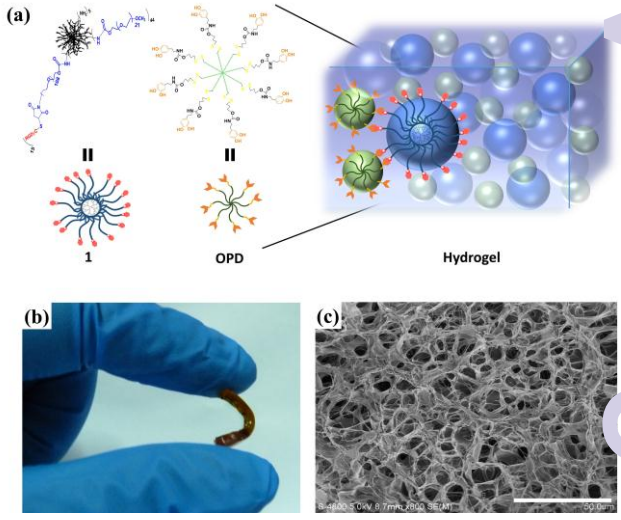

Fig. 1. (a) Schematic description of the hydrogel from **1** and **OPD**. (b) Photograph of the hydrogel at room temperature. (c) SEM image of the hydrogel with scale bar of 50 μm. The hydrogel was prepared from **1/OPD** (at a 1/2 ratio, **OPD**: 15% (w/v)) and fully swelled at 37°C after 48 h.

[a] *Beijing National Laboratory for Molecular Sciences (BNLMS), College of Chemistry and Molecular Engineering, Peking University, Beijing 100871, P. R. China, Email: xrjia@pku.edu.cn;*
[b] *Key Laboratory of Polymer Chemistry and Physics of the Ministry of Education, Peking University, Beijing 100871, P. R.China;*
[c] *State Key Laboratory for Structural Chemistry of Unstable and Stable Species, Peking University, Beijing 100871, P. R. China;*
[d] *Chongqing Key Laboratory for Oral Diseases and Biomedical Sciences Chongqing Municipal Key Laboratory of Oral Biomedical Engineering of Higher Education, Chongqing 400016, P. R. China, Email:ysdentist@hotmail.com;*
[e] *Department of Chemistry, Tsinghua University, Beijing 100084, P. R. China.*
† Footnotes relating to the title and/or authors should appear here.
Electronic Supplementary Information (ESI) available: [details of any supplementary information available should be included here]. See DOI: 10.1039/x0xx00000x

applications as a result of their size reaching to nano-objects with dimensions similar to nature proteins.[15] Several examples have proved that the dendrimer-based hydrogels are of great values as drug delivery carriers.[16] However, limited reports deal with the hydrogels from dendrimers for potential applications in tissue engineering,[17] such as the skeletal tissue regeneration, the replacement of bone and cartilage, etc. The previous study showed that PAMAM molecules, in particular, the higher generations played a key role in upgrading the nature of hydrogels.[18] The well-defined architecture and the easily functionalized periphery groups of PAMAM dendrimers make them an excellent new type of cross-linking agent for fabricating the gel phase networks with more compact structure.

Inspired by previous results mentioned above, we designed and produced a high performance hydrogel by integrating two nanosphere-like components, a bioactive fragment modified G4.0 PAMAM dendrimer (named **1**) and a DOPA-terminated 8-armed PEG (named **OPD**). The superiorities of the hydrogel from these two components are believed: (1) the multi-branched and sphere-like topology of PAMAM molecules may provide more cross-linking sites to construct a dense cross-linking network with a possible cross-linking homogeneity in the gelation process; (2) the strong interfacial adhesion strength of DOPA may provide the hydrogel with enhanced adhesion to tissue and increased mechanical strength; and (3) the biocompatibility and bioactivity of the peptides modified on the periphery of PAMAM molecules may meet the requirements to implant in the physiological environment. As expected, the obtained hydrogel showed much higher mechanical strength, low and stable swelling ratio and biodegradable properties. The two components, in particular the nanosized sphere-like PAMAM dendrimers, showed noteworthy influence on reducing the hydrogel's swelling and enhancing the mechanical stiffness. Furthermore, the in vitro test evidenced that the hydrogel exhibited good biocompatibility with no cytotoxicity. The mouse calvarial critical size defect (CSD) model assay in vivo demonstrated the possibility of the hydrogel used for bone regeneration. To the best of our knowledge, this is a rare report of a high performance hydrogel from the combination of two nanosphere-like components of PAMAM dendrimer and DOPA-terminated 8-armed PEG.

Fig. 1a depicts the fabrication of the hydrogel from the two nanosphere-like components. For the dendritic component **1**, we initially connected maleimide-PEG-succinimidyl carbonate ester (MAL-PEG5000-NHS) and methoxy-PEG-succinimidyl carbonate ester (mPEG1000-NHS) on the surface of PAMAM molecules. It aimed to enhance the biocompatibility and dissolution properties, and to covalently conjugate the bioactive peptide of arginine-glycine-(aspartic acid)-(D-tyrosine)-cysteine (RGDyC) through an effective Michael addition reaction (Scheme S1). The symbols "y" and "C" in the abbreviation of RGDyC represent the crosslinkable group of D-tyrosine and the thiol group of cysteine used for grafting with PEG, respectively. Another component, **OPD** was prepared by reacting thiol-terminated-8-armed PEG with 4-nitrophenyl (3-(pyridin-2-yldisulfanyl) propyl) carbonate activated dopamine hydrochloride (Scheme S2). For a comparison, the hydrogels from **OPD** alone and from G4.0 PAMAM dendrimers with PEG and arginine-alanine-alanine-(aspartic acid)-(D-tyrosine)-cysteine (RAADyC) fragments on the surface (named **2**, Scheme S1) were synthesized as the control samples. The cross-linking networks were fabricated via an oxidation-induced reaction mainly between the catechol groups of **OPD** and the phenol groups of RGDyC on the periphery of **1** in the presence of $NaIO_4$, from which a degradable hydrogel could be achieved because of the disulfide bonds in the structure of **OPD**.

^{1}H NMR measurements were carried out to quantify the grafting ratio of DOPA units on **OPD** and of mPEG and RGDyC on the periphery of G4.0 PAMAM molecules. It showed that each arm of 8-armed PEG (MW 20 kDa) was ended by a DOPA unit (Fig. S1), and that about 15 RGDyC groups and 44 mPEG1000 moieties (for **1**), 14 RAADyC groups and 45 mPEG1000 moieties (for **2**) were conjugated onto the exterior of each PAMAM molecule (Fig. S2). These results indicated that the conjugating reaction for modifying PAMAM molecules was quantitatively controlled with high efficiency. The UV-Vis, FT-IR and Differential scanning calorimetry (DSC) measurements were performed (Fig. S3, S4 and S5). The results of distinct crystallization temperatures (T_c) and melting points (T_m) of 8-armed PEG, **OPD**, G4.0 PAMAM, **1** and **2** supported the ^{1}H NMR data. The detailed synthetic procedures and characterizations of **OPD**, **1** and **2** are described in the Supporting Information.

For affording a robust gel, **OPD** was screened in a range of concentrations from 5% to 20% (w/v), and the mass ratios of **1/OPD** were explored within 1/10, 1/5 and 1/2 (Table S1 and S2). As a result, we found that **OPD** was essential for the gelation. No hydrogel but nanogel was observed by dendritic component **1** alone (Fig. S6), indicating that the two components connected alternately with each other to construct the porous networks. It was established that the tough hydrogel could be obtained with the concentration of **OPD** at 15% and the ratio of **1/OPD** in 1/2 (Fig. 1b). Besides, the gelation time could be controlled from several minutes to half an hour by adjusting the amount of **OPD** and $NaIO_4$.

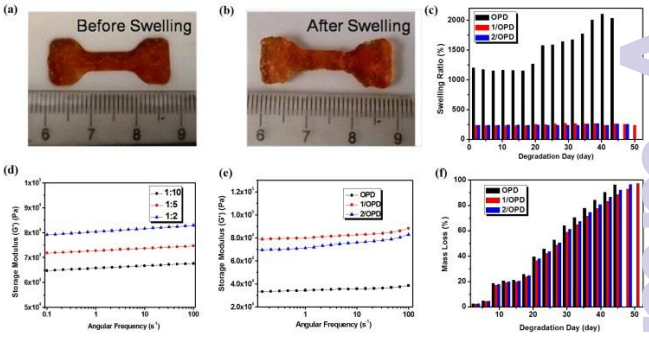

Fig. 2. Photographs of the hydrogel (a) before (b) after swelling at 37°C after 48 h. (c) Equilibrium swelling ratio of **OPD** alone, **1/OPD** and **2/OPD** at the ratio of 1/2, measured on the indicated days. Plots of the angular frequency (ω) versus storage modulus (G') of (d) **1/OPD** hydrogels with different ratios; and (e) **OPD** alone, **1/OPD** and **2/OPD** hydrogels at the ratio of 1/2 (measured at a strain of 10%). All the samples involved were fully swelled at 37°C after 48 h. (f) Degradation of hydrogels from **OPD**, **1/OPD** and **2/OPD** at the ratio of 1/2. The complete degradation period in PBS buffer is 45, 51 and 4[illegible] day, respectively. Concentration of GSH: 4 μM, **OPD**: 15% (w/v)

Porous hydrogels with the pores sizes ranging from submicron to micro are ideal for maintaining cell activity and nutrient exchange. The interconnected 3D pore networks can also provide an ideal environment for tissue growing and cell adhering and proliferating.[19] We performed scanning electron microscopy (SEM) measurement to visualize and confirm the gel phase structure of **1/OPD**. The gel phase networks exhibited a highly permeable interconnected porous morphology with a rather dense and refined porous structure (Fig. 1c, S7a and S7b). The networks were composed of numerous small holes with the sizes ranging from 5 μm to 30 μm. The similar structure could also be found for **2/OPD** (Figure S7c). It might be due to the sphere-like topology, flexible conformation and multi-branched structure of the two components, which facilitated them to contact each other and densely cross-linked.

The suppression of swelling is regarded as an efficient strategy to attain a tough hydrogel.[20] In the swelling property examination of **1/OPD** hydrogel, **1** displayed more prominent impact on lowering and stabilizing the hydrogel's swelling (Fig. 2a, 2b and 2c). As compared to a swelling ratio beyond 1500% for the hydrogel consisting of only **OPD**, **1/OPD** hydrogel dramatically reduced the swelling ratio to below 248% (Table S3). As shown in Fig. 2a and 2b, it is visible that not only the gel's volume but also its shape were well-maintained after the sample was fully swelled. This result illustrates the "dendritic effect" of PAMAM molecules, which act as the discrete multivalent junction points to scaffold the networks and suppress the swelling. The less swelling property is beneficial to retain the strength of the hydrogels and highly encounters the criteria in clinical applications such as surgery usage for avoiding the applied hydrogel to exceed the trauma boundaries and detach from the wound sites.

The rheological behaviors such as storage modulus G', loss modulus G'' (Fig. S8) and compressive modulus were measured to assess the mechanical stiffness of the hydrogel. The robust hydrogel was obtained as a result of mixing **1** and **OPD** at the mass ratio of 1/2, otherwise lower G' values were observed (Fig. 2d). The G' value of **1/OPD** hydrogel achieved 84 kPa, much higher than the hydrogel from **OPD** alone (36 kPa) (Fig. 2e, S9, and Table S4). The compressive modulus of **1/OPD** hydrogel also increased to about 30 kPa that was superior to **OPD** hydrogel (Fig. S10 and Table S5). This observation results in the following conclusions. (1) The stiffness of the hydrogel may mainly ascribe to the high cross-linking density owing to the PAMAM dendrimers with multiple cross-linking sites on the periphery. Increasing the crosslinking density has been reported in recent advances as an efficient strategy to reach the mechanical properties of native tissue.[17] (2) The DOPA residues in **OPD** are crucial for enhancing the mechanical strength of the hydrogel as compared with other hydrogels made from eight armed PEG polymers.[21] This result is also consistent with the report of Messersmith et al.,[14] who found that the G' value of hydrogels crosslinked by DOPA was much higher than the ones without DOPA. (3) The nanosphere-like components of **1** and **OPD** are unlike the conventional building blocks in the hydrogel systems. We assume that the two multi-branched components, in particular, the dendritic architecture of **1** is likely to be the impenetrable nanospheres having the non-entangling nature in solution. Such property may conduce to less inhomogeneous distribution of cross-links in the gel phase. This situation is possibly similar to the 'non-swellable' gel system from two tetra-armed PEG polymers with high mechanical strength and toughness.[20b]

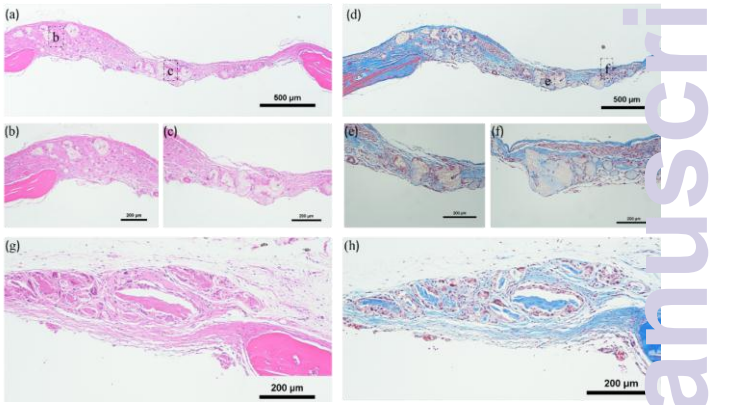

Fig. 3. Histology of treated bone defect with **1/OPD** hydrog after 4 weeks (a-f) and 6 weeks (g, h). H&E (a-c, g) and Masson's trichrome staining (d-f, h) were applied to show the defect repair. **1/OPD** is at the ratio of 1/2 and the concentration of **OPD** is 15% (w/v).

The hydrogels were degradable through the breakage of disulfide bonds by glutathione (GSH) at different concentrations, which is a common way to be applied for mimicking ECM and bone regeneration.[22] All the hydrogels could gradually degrade in 50 da in the presence of 4 μM GSH (Fig. 2f), while maximizing th concentration to 10 mM, the hydrogel immediately degraded t become a liquid (Fig. S11), indicating a controllable manner o degradation corresponding to the concentration of GSH in th physiological environment.

For the hydrogel of **1/OPD**, evidence of cell toxicity was no observed within the 72 h in vitro by showing more cell viability tha the control samples of **OPD** and **2/OPD** when the mouse bon marrow mesenchymal stem cells (mMSCs) were incubated in the hydrogels (Fig. S12). Moreover, the mouse calvarial critical ze defect (CSD) model was constructed to preliminarily test the possibility of the hydrogel for bone regeneration in vivo. No noticeable toxic side effects were found after implantation of th **1/OPD** hydrogel into the surgery sites of mice in 6 weeks. All th mice recovered well with the body weight remained stable and n visible signs of head unhairing. Micro-CT (μCT) measurement revealed that moderate new bone-like tissue and extensive bon tissue were observed in 4 weeks and in 6 weeks in the **1/OPD** mic group (Fig. S13). Histological analysis supported the enhanced bone formation in **1/OPD** mice group. It showed the preosteoblastic-lik cells lining on the newly formed bone tissue with osteocytes embedded within lacuna from H&E staining (Fig. 3a, 3b, 3c, 3g, S14a, S14b and S14e). The woven bone tissues at the peripheral of de ct and also in the center of graft were presented from Masson's thrichrome staining (Fig. 3d, 3e, 3f, 3h, S14c, S14d and S14f).

In conclusion, we constructed a new biodegradable hydrogel b combining two components of a bioactive fragmnets modified G4.0 PAMAM and a DOPA-terminated-8-armed PEG, which exhibited a excellent interconnected porous 3D network structure, a higher mechanical strength, a low and stable swelling ratio, wo biocompatibility and in vivo performance of a scaffold for mouse

cranial defect repair. This dendrimer-based hydrogel may serve as a model for potential clinical applications and provide a new way for developing advanced biomaterials in tissue engineering.

Acknowledgements

This work is financially supported by the National Natural Science Foundation of China (21174005 and 21274004) to X.-R. Jia. It is also financially supported by the National Natural Science Foundation of China (81500894) and the Specialized Research Fund for the Doctoral Program of China (SRFDP20125503120009) to S. Yang.

Notes and references

1 (a) J. Kisiday, M. Jin, B. Kurz, H. Hung, C. Semino, S. Zhang and A. J. Grodzinsky, *Proc. Natl. Acad. Sci. USA,* 2002, **99**, 9996-10001; (b) J. K. F. Suh and H. W. T. Matthew, *Biomaterials,* 2000, **21**, 2589-2598.
2 (a) S. J. Bryant and K. S. Anseth, *J. Biomed. Mater. Res.,* 2002, **59**, 63-73; (b) T. P. Kraehenbuehl, P. Zammaretti, A. J. Van der Vlies, R. G. Schoenmakers, M. P. Lutolf, M. E. Jaconi and J. A. Hubbell, *Biomaterials,* 2008, **29**, 2757-2766.
3 (a) K. Y. Lee and D. J. Mooney, *Chem. Rev.,* 2001, **101**, 1869-1879; (b) J. L. Drury and D. J. Mooney, *Biomaterials,* 2003, **24**, 4337-4351.
4 (a) B. Jeong, Y. H. Bae, D. S. Lee and S. W. Kim, *Nature,* 1997, **388**, 860-862; (b) R. Censi, P. Di Martino, T. Vermonden and W. E. Hennink, *J. Control. Release,* 2012, **161**, 680-692.
5 (a) B. V. Slaughter, S. S. Khurshid, O. Z. Fisher, A. Khademhosseini and N. A. Peppas, *Adv. Mater.,* 2009, **21**, 3307-3329; (b) C.-C. Lin and K. S. Anseth, *Pharm. Res.,* 2009, **26**, 631-643.
6 (a) T. J. Klein, S. C. Rizzi, J. C. Reichert, N. Georgi, J. Malda, W. Schuurman, R. W. Crawford and D. W. Hutmacher, *Macromol. Biosci.,* 2009, **9**, 1049-1058; (b) J. Malda, J. Visser, F. P. Melchels, T. Juengst, W. E. Hennink, W. J. A. Dhert, J. Groll and D. W. Hutmacher, *Adv. Mater.,* 2013, **25**, 5011-5028.
7 (a) D. Seliktar, *Science,* 2012, **336**, 1124-1128; (b) B. L. Seal, T. C. Otero and A. Panitch, *Mater. Sci. Eng., R,* 2001, **34**, 147-230.
8 Y. Okumura and K. Ito, *Adv. Mater.,* 2001, **13**, 485-487.
9 K. Haraguchi and T. Takehisa, *Adv. Mater.*, 2002, **14,** 1120-1124.
10 J. P. Gong, Y. Katsuyama, T. Kurokawa and Y. Osada, *Adv. Mater.,* 2003, **15**, 1155-1158.
11 (a) J. A. Burdick and K. S. Anseth, *Biomaterials,* 2002, **23**, 4315-4323; (b) L. A. S. Callahan, A. M. Ganios, D. L. McBurney, M. F. Dilisio, S. D. Weiner, W. E. Horton Jr., and M. L. Becker, *Biomacromolecules,* 2012, **13**, 1625-1631.
12 T. Huang, H. Xu, K. Jiao, L. Zhu, H. R. Brown and H. Wang, *Adv. Mater.,* 2007, **19**, 1622-1626.
13 (a) H. Lee, N. F. Scherer and P. B. Messersmith, *Proc. Natl. Acad. Sci. USA,* 2006, **103**, 12999-13003; (b) H. Lee, B. P.Lee and P. B. Messersmith, *Nature,* 2007, **448**, 338-341; (c) J. H. Waite and J. N. Israelachvili, *Proc. Natl. Acad. Sci. USA,* 2007, **104,** 3782-3786.
14 (a) J. L. Dalsin and P. B. Messersmith, *Biomacromolecules,* 2002, **3**, 1038-1047; (b) C. E. Brubaker and P. B. Messersmith, *Biomacromolecules,* 2011, **12**, 4326-4334; (c) B. P. Lee and S. Konst, *Adv. Mater.,* 2014, **26**, 3415-3419.
15 (a) C. C. Lee, J. A. MacKay, J. M. J. Fréchet and F. C. Szoka, *Nat. Biotechnol.,* 2005, **23**, 1517-1526; (b) S. Svenson and D. A. Tomalia, *Adv. Drug Deliv. Rev.,* 2005, **57**, 2106-2129.
16 (a) H. He, Y. Li, X.-R. Jia, J. Du, X. Ying, W.-L. Lu, J.-N. Lou and Y. Wei, *Biomaterials*, 2011, **32**, 478-487; (b) Y. Li, H. He, X. Jia, W.-L. Lu, J. Lou and Y. Wei, *Biomaterials*, 2012, **33**, 3899-3908; (c) H. He, Y. Wang, H. Wen and X. Jia, *Rsc Adv.*, 2014, **4**, 3643-3652.
17 (a) S. H. M. Sontjens, D. L. Nettles, M. A. Carnahan, L. A. Setton and M. W. Grinstaff, *Biomacromolecules,* 2006, **7**, 310-316; (b) L. Degoricija, P. N. Bansal, S. H. M. Sontjens, N. S. Joshi, M. Takahashi, B. Snyder and M. W. Grinstaff, *Biomacromolecules,* 2008, **9**, 2863-2872.
18 Y. Wang, Q. Zhao, H. Zhang, S. Yang and X. Jia, *Adv. Mater.*, 2014, **26**, 4163-4167.
19 V. Karageorgiou and D. Kaplan, *Biomaterials,* 2005, **26**, 5474-5491.
20 (a) T. Sakai, T. Matsunaga, Y. Yamamoto, C. Ito, R. Yoshida, S. Suzuki, N. Sasaki, M. Shibayama and U.-i. Chung, *Macromolecules*, 2008, **41**, 5379-5384; (b) H. Kamata, Y. Akagi, Y. Kayasuga-Kariya, U.-i. Chung and T. Sakai, *Science*, 2014, **343**, 873-875.
21 (a) C. Hiemstra, Z. Y. Zhong, L. B. Li, P. J. Dijkstra and J. Feijen, *Biomacromolecules*, 2006, **7**, 2790-2795; (b) S. J. Buwalda, P. J. Dijkstra, L. Calucci, C. Forte and J. Feijen, *Biomacromolecules*, 2010, **11**, 224-232.
22 (a) F. Yang, J. Wang, J. Hou, H. Guo and C. Liu, *Biomaterials*, 2013, **34**, 1514-1528; (b) J. Madsen, S. P. Armes, K. Bertal, H. Lomas, S. MacNeil and A. L. Lewis, *Biomacromolecules*, 2008, **9**, 2265-2275; (c) H.-W. Chien, W.-B. Tsai and S. Jiang, *Biomaterials*, 2012, **33**, 5706-5712.